sustainability

MDPI

Article

The Natural Attenuation of Bioavailable Sulfur Loads in Soil Around a Coal-Fired Power Plant 20 Years After Ceasing Pollution: The Case of Plomin, Croatia

Neža Malenšek Andolšek [1,*], Sonja Lojen [2,3] and Nina Zupančič [4,5]

[1] Department of Mineral Resources and Geochemistry, Geological Survey of Slovenia, Dimičeva ulica 14, 1000 Ljubljana, Slovenia
[2] Department of Environmental Sciences, Jožef Stefan Institute, Jamova 39, 1000 Ljubljana, Slovenia; sonja.lojen@ijs.si
[3] School of Environmental Sciences, University of Nova Gorica, Vipavska cesta 13, 5000 Nova Gorica, Slovenia
[4] Department of Geology, Faculty of Natural Sciences and Engineering, University of Ljubljana, Aškerčeva 12, 1000 Ljubljana, Slovenia; nina.zupancic@ntf.uni-lj.si
[5] Ivan Rakovec Institute of Paleontology, The Research Centre of the Slovenian Academy of Sciences and Arts, 1000 Ljubljana, Slovenia
* Correspondence: neza.malensek@geo-zs.si

Abstract

The coal-fired Plomin Thermal Power Plant (Plomin TPP) in Croatia is located in the center of the east coast of the Istrian peninsula (northern Adriatic) and is considered the main source of historical air pollution in the region. Between 1970 and 2000, sulfur-rich coal from the local Raša coal mine was primarily used. In this study, a screening of content and fate of TPP-derived sulfur in soil around the power plant was made two decades after the S-rich coal was banned from use. Soil samples were collected at varying distances from the TPP in the prevailing wind direction (NE), along with a control sample taken more than 10 km away. The samples were analyzed for total sulfur, sulfate, organic sulfur (humic and fulvic), and the stable isotope composition of total sulfur ($\delta^{34}S$). Additionally, coal and coal ash were analyzed for total sulfur, sulfate and $\delta^{34}S$. Soil sampling along the prevailing wind direction from the Plomin TPP revealed markedly elevated sulfur content, with levels at 100 m downwind reaching up to 4 wt.%, which is over 100 times higher than the 0.04 wt.% measured at the control site located upwind. Sulfur content decreases sharply with increasing distance from the TPP, reflecting the deposition gradient along the prevailing wind path. Speciation analysis showed that over 95% of the sulfur in the soil is now present in organic form, mainly bound to humic acids. The $\delta^{34}S_{VCDT}$ values of the bulk coal used in the TPP ranged from −10.0 to −5.0‰. In most soil samples, the bulk $\delta^{34}S$ values were positive (+7.0 to +20.0‰). The values of sulfate in soil range from +1.0 to +5.5‰, while those in organic sulfur range from −3.5 to +6.0‰. This indicates that atmospheric deposition of ^{34}S-depleted fly ash and sulfate from coal are the most important sulfur sources, while some of the sulfur in the soil is also of marine origin. Finally, we showed that natural attenuation was a significant and efficient process within the sustainable management of the site historically contaminated by anthropogenic atmospheric sulfur deposition.

Keywords: historical pollution; soil; sulfur; stable isotopes; thermal power plant; coal; natural attenuation

Academic Editor: Guannan Liu

Received: 20 November 2025
Revised: 24 December 2025
Accepted: 8 January 2026
Published: 12 January 2026

1. Introduction

Soil is the most biologically and biochemically active environmental compartment and therefore plays a pivotal role in the biogeochemical cycles of all bioactive elements, including sulfur (S). Sulfur is one of the most important elements in nature and represents between 0.03 and 0.1 wt.% of the Earth's crust [1,2]. The total S content in soil typically ranges from 0.01 to 0.1%, most of which is inaccessible to organisms [3]. The most important S reservoirs in soil are organic matter, minerals derived from the weathering of bedrock (e.g., pyrite, gypsum), and sulfate from atmospheric deposition. Anthropogenic input is also significant, either as contamination or through fertilization [4].

Despite its negative environmental impacts, coal remains one of the most important energy sources in many parts of the world, providing about one-third of global electricity generation [5]. Coal combustion typically produces sulfur dioxide (SO_2), nitrogen oxides (NO_X), carbon dioxide (CO_2), and increases the content of various potentially toxic trace elements (e.g., As, Cd, Cr, Hg, Ni, Se, and V), as well as organic pollutants such as polycyclic aromatic hydrocarbons (PAHs). Therefore, it is one of the most significant anthropogenic sources of sulfur input into soil.

In Croatia, the Plomin coal-fired Thermal Power Plant (TPP) has been in operation since 1970 and is the country's only active coal-fired facility. It is located in the small town of Plomin, which has only 124 residents, at the tip of Plomin Bay, just 3.5 m above sea level, and features a 340-meter-high stack. The plant has been a significant source of electricity, contributing around 13% of the country's total electricity production [6]. Between 1970 and 2000, the local super-high organic sulfur Raša coal was burned, with sulfur concentrations of up to 12% [7–10], causing environmental pollution. Over 30 years, Raša coal combustion is estimated to have emitted nearly 8.5 tons of SO_2 per hour of operation, far exceeding the World Bank's recommended limit of 1 ton per hour for plants of similar capacity [10].

The environmental impact of sulfate aerosols from the plant has been substantial, affecting air quality, soil, water, and human health. Prior to modern emission controls, Raša coal combustion resulted in elevated levels of airborne contaminants and trace metals in surrounding ecosystems. For decades, the dominant northeast Bora winds have spread industrial fumes, especially SO_2 and airborne particles, contaminating the area. Additionally, Raša coal combustion produced 10^6 tons of waste ash, deposited over 120,000 m^2 near the facility and later dispersed in considerable amounts by wind [11]. Concerns about potential environmental threats are augmented because of the karstic terrain, which is highly sensitive to contamination due to the high permeability of rocks and their connection to groundwater. Although more than two decades have passed since local coal was replaced by imported low-sulfur coal, the consequences of the long-term use of Raša coal and the improper implementation of remediation measures (such as scattering ash in the surrounding area) are still noticeable in the environment [12–14]. The long-term fate of sulfur in the soil remains poorly understood.

Since then, numerous studies have investigated the environmental and health impacts of the Plomin TPP. These include assessments of heavy metals in soil [15,16], health risk from Plomin Bay sediments [17], radioactivity levels in the area [11], and health correlations with SO_2 exposure [18,19]. Additional research has examined sulfur accumulation in pine needles [20]. Further studies have analyzed the distribution of polycyclic aromatic hydrocarbons (PAHs) and trace elements in soil [12,14,21], radionuclide distribution [13], and the mobility of toxic elements from combustion by-products [10]. Soils near the Plomin TPP have been found to contain elevated levels of sulfur (up to 3%), PAHs (up to 13,535 ng/g), potentially toxic metals (including uranium), ^{226}Ra (up to 580 Bq/kg), and other pollutants [10,12–14].

Historical sulfur deposition can persist in soils long after emissions cease, but total sulfur alone may not reflect true environmental risk. Much of this sulfur is stabilized in organic or mineral-associated forms, which are less bioavailable but can be remobilized over time. Natural attenuation, through microbial sulfurization and plant recycling, helps stabilize sulfur and reduce long-term impact. Understanding natural attenuation processes is therefore essential for long-term risk assessment, the development of smart monitoring plans, and smart environmental management strategies, such as avoiding unnecessary remediation interventions with low added efficiency and potentially higher carbon footprints.

The aim of the study is to determine the spatial distribution of sulfur and its isotopes in soil at various distances from the power plant in the wind direction, to identify its source and the nature of its occurrence 20 years after the cessation of massive SO_4^{2-} emissions from the Plomin TPP, and to investigate the processes influencing its changes over time. We hypothesize that total sulfur content in soils is highest near the former emission source and decreases with distance. Over the past two decades, we further expect a general decline in total sulfur content, accompanied by a shift from more mobile sulfate forms to more stable, mineral-associated and organically bound sulfur. Consequently, we expect sulfur speciation, rather than total sulfur content alone, to better reflect long-term environmental risk and the potential for further remobilization.

2. Materials and Methods

2.1. Study Area

The Plomin TPP is located near the village of Plomin, close to Plomin Bay on the Istrian peninsula in the northern Adriatic, Croatia (Figure 1). The study area is part of the classic karst region [22,23]. It lies within the Adriatic carbonate platform [24], which existed during the Mesozoic era and consists of Cretaceous shallow-water dolomites and limestones covered with rendzina and terra rossa soils [16,25]. One of the main characteristics of this area is the presence of bituminous coal beds.

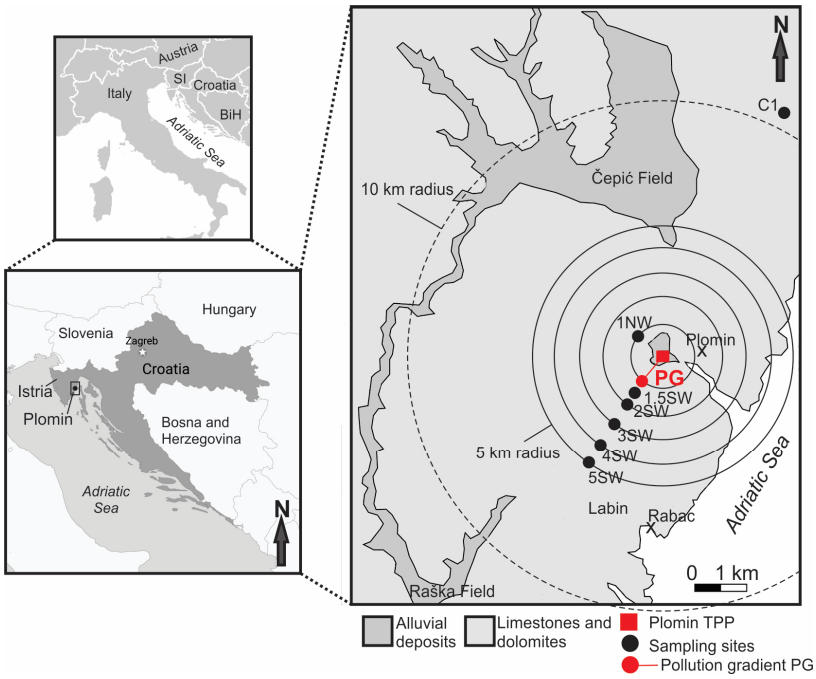

Figure 1. Location of the Plomin area, simplified lithological map of the study area and sampling scheme.

The climate in this area is Mediterranean, with mild, humid winters and hot, dry summers. The average annual rainfall is 1294 mm. The prevailing wind directions around Plomin TPP are northeast (NE) and east-northeast (ENE) (Figure 2). Strong Bora winds frequently occur in Plomin, Istria, with average speeds ranging from approximately 40 km/h to over 100 km/h and extreme gusts occasionally reaching 160 km/h during strong events. [26]. The vegetation of the Istria Peninsula reflects the region's transitional position between Mediterranean and continental climate zones and its predominantly karstic geology. The landscape is characterized by a mixture of deciduous forests, grassland, and arable land with Mediterranean-type vegetation predominant in the coastal areas. The town of Labin is located 5–8 km southwest (SW) of the Plomin TPP. In addition to its unsuitable location on vulnerable karst terrain, which is covered by a thin layer of soil, the prevailing northeasterly (NE) winds carry airborne pollutants and ash directly from the Plomin TPP to the town of Labin.

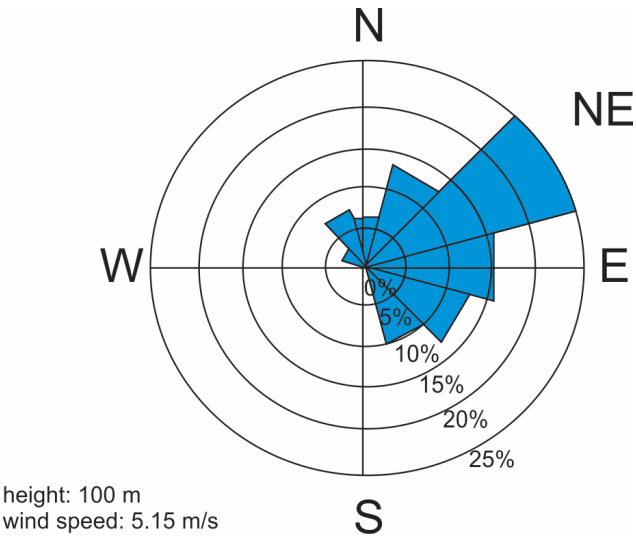

Figure 2. Wind rose showing the long-term (2008–2017) prevailing wind direction in the study area, derived from a regional wind atlas [26] based on multi-year meteorological observations. NE dominance reflects average conditions, not a unidirectional wind [26].

2.2. Sampling

A total of 20 samples were analyzed, including 12 soil samples (Table 1), 3 ash samples, and 6 samples of Raša coal. The ash, coal and some soil samples (19, 20, 21, 22, 28 and C1) were the same as those analyzed by Medunić et al. [12,14]. Nine soil samples were collected at different distances along the prevailing wind direction (SW) from the Plomin TPP and at approximately the same distance from the Adriatic Sea. In contrast, the control soil sample (C1) was taken more than 10 km away from the Plomin TPP in the NE wind direction (Figure 1). Four samples (20, 21, 22 and 28) were taken along the pollution gradient (PG) at distances between 100 m and 1 km from the Plomin TPP [12]. The rest of the soil was sampled in the same direction at distances of 1.5 km, 2 km, 3 km, 4 km, and 5 km. To verify the assumption that the S content would be higher in the prevailing wind direction (NE–SW), a soil sample was also taken in the northwest (NW) direction, 1 km from the Plomin TPP. At each site, about 2 kg of the upper part of the soil without organic horizon, was taken. Some samples were taken from molehills.

Table 1. Soil samples, their distances from the Plomin TPP and coordinates (Google Earth).

Sample	Distance (m)	N	E
19	100	45°8′2.6″	14°9′27.4″
20	200	45°8′0.4″	14°9′23.3″
21	300	45°7′58.1″	14°9′19.3″
22	400	45°7′55.6″	14°9′16.2″
28	1000	45°7′42.1″	14°8′51.8″
1.5 KM (SW)	1500	45°7′28.2″	14°9′3.7″
2 KM (SW)	2000	45°7′20.2″	14°8′48.8″
3 KM (SW)	3000	45°6′55.12″	14°8′20.5″
4 KM (SW)	4000	45°6′28.3″	14°8′7.9″
5 KM (SW)	5000	45°6′10.5″	14°8′24.6″
1 KM (NW)	1000	45°8′50″	14°9′15.2″
C1	>10,000	45°14′29.32″	14°15′18.66″

2.3. Sample Preparation

The total S concentrations and their stable isotope composition were analyzed in coal, coal ash, and soil samples. In addition, S bound in sulfate, humic and fulvic acids were extracted from the soil and analyzed for its concentration. The isotopic composition of S was determined in bulk soil samples and extracts where sufficient material was obtained for isotope analysis. Sulfides in coal were not considered, as it was assumed they are oxidized during coal combustion in the presence of air.

All the samples were first dried in an oven at 60 °C, crushed in an agate mortar and sieved (160 μm).

As the sulfate is water-soluble, it was extracted from the dry soil by a wet chemical procedure [27], summarized in Figure 3. First, the dry samples were weighed and mixed with Milli-Q water at a mass ratio of 1:10. The samples were then stirred with a mechanical stirrer for two hours and left to rest for 24 h. After 24 h, the samples were vacuum filtered through GFF glass-fiber filters (Whatman, Maidstone, UK). The pH of the filtrate was reduced to <2 by adding 10% HCl (p.a., Carlo Erba, Cornaredo, MI, USA), and 10 mL of 10% $BaCl_2$ (Merck, Darmstadt, Germany, 99%) was added to precipitate the sulfate as $BaSO_4$. The suspension was heated to boiling temperature and then left to settle for 24 h. The precipitate was washed several times with Milli-Q water and filtered through a 0.45 μm nylon mesh filter (Millipore, Burlington, MA, USA). The sediment remaining after elution of the sulfate was dried, crushed, and stored for further analysis. To extract the humic and fulvic compounds, the sediment was dispersed in 1 L of 0.1 M NaOH solution, shaken for 7 days, and filtered (GF/F). The humic compounds were precipitated by adding HCl to a pH < 2, settled for 24 h, filtered, washed with Milli-Q water, and freeze-dried. The filtrate was heated to boiling and amended with 20 mL of H_2O_2 (p.a., 30%, Merck) to oxidize the fulvic-bound S to SO_4^{2-}. After 90% of the volume had evaporated, 10 mL of 10% $BaCl_2$ was added, and the $BaSO_4$ was isolated as described above [27,28].

The extraction of total S from coal and the humic fractions of the soil was carried out according to a standard procedure by combustion with Eschka mixture [29]. First, the samples were homogeneously mixed with an equal amount of Eschka mixture (Sigma–Aldrich Chemie GmbH, Steinheim, Germany). They were then placed in refractory crucibles, with the bottoms covered by a layer of Eschka mixture about 5 mm thick, followed by another layer of Eschka on top. The samples were annealed for two hours at 800 °C and then slowly cooled overnight. The sulfate produced was then recovered as $BaSO_4$ as previously described [27].

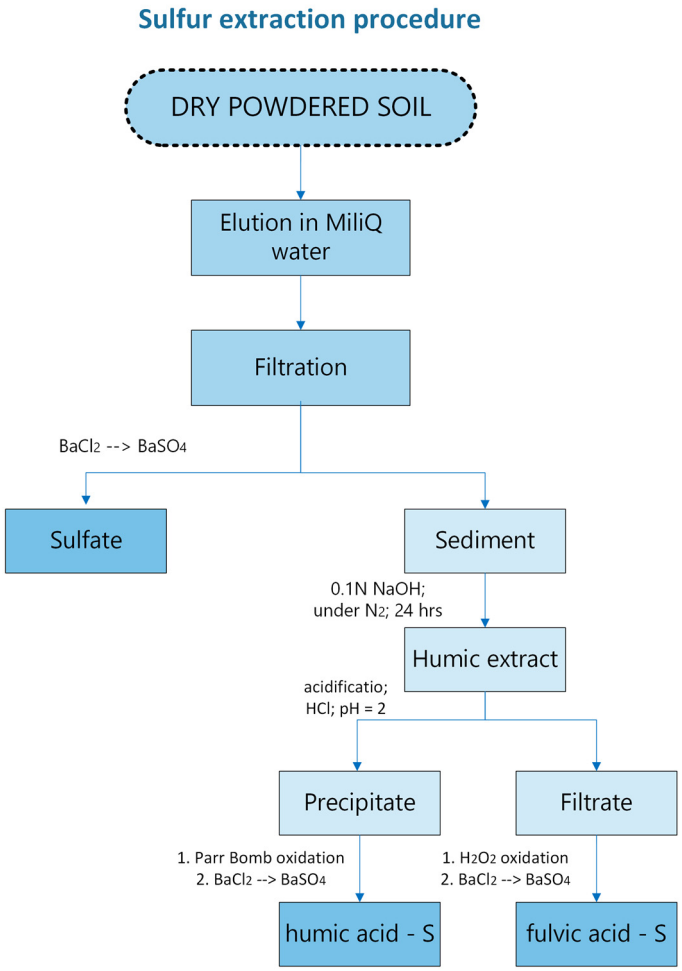

Figure 3. Sulfur extraction procedure.

2.4. Analyses

The X-ray diffraction method, conducted at the Faculty of Natural Science and Engineering, Department of Geology, Slovenia, was used to determine the mineral composition of soil, ash, and coal samples. The diffraction patterns were identified with X'Pert HighScore Plus 4.6a software using the PAN-ICSD database and Rietveld refinement, using the Pseudo-Voigt function for rough semi-quantitative mineral phase analysis.

The S concentration in bulk samples 20, 21, 22, 28, and C1 was measured using the PIXE (Particle-Induced X-ray Emission) method performed at the Rudjer Bošković Institute Tandem Accelerator Facility, Croatia [12]. The S content in other bulk samples and the isotopic composition of S was determined by isotope ratio mass spectrometry (EA-IRMS, IsoPrime 100 with PyroCube, Elementar Analysensysteme GmbH, Langenselbold, Germany) at the Jožef Stefan Institute, Slovenia. Aliquots of 0.5 mg of sample extracts ($BaSO_4$) were weighed into tin capsules (Secron, Crewe, UK, 6 × 4 mm) and mixed with three times the amount of WO_3. Combustion occurred in the elemental analyzer's oxidation column, maintained at 1075 °C, with a jet-injection of oxygen (4.8), ensuring the decomposition temperature exceeded 1400 °C. The samples were quantitatively converted to SO_2, purified in two gas-selective columns, and introduced into the isotope-ratio mass spectrometer. Helium (0.6) was used as the carrier gas. The raw data were processed using IonVantage software for IsoPrime (2014). Reproducibility of replicates for the entire wet extraction procedure and Eschka combustion extraction was within 10%, with the measured for S isotopic composition falling within the overall measurement uncertainty.

Measurement data were recalculated to $\delta^{34}S$ values, representing the deviation of the $^{34}S/^{32}S$ ratio of the sample from that of the standard, expressed in per mil (‰), and calibrated to the VCDT (Vienna- Cañon Diablo Troilite) scale using the USGS Laboratory Management System (LIMS) for light isotopes [30]. Two calibration materials were used: IAEA-SO-6 and NBS-127 $BaSO_4$, with certified $\delta^{34}S_{VCDT}$ values of −34.12 and +21.7‰, respectively [31]. Analytical quality was controlled and assured by analyzing certified reference material as controls (accuracy) and replicate measurements (precision). As controls, the Protein (Casein) Standard OAS and IAEA-SO-5 ($BaSO_4$) certified reference materials with $\delta^{34}S_{VCDT}$ values of +6.18 and +0.5‰, respectively, were used. Calibration materials and test samples were randomly dispersed in each sample batch. All samples and reference materials were analyzed in triplicate, and results were accepted if the standard deviation of replicate measurements was within the long-term uncertainty of control material measurements (0.2‰). If the standard deviation was larger, analyses were repeated until the required precision was achieved. Obtained analytical results meet the standard analytical quality. The detection limit for analyses cannot be determined universally and depends on the sample and type of analysis. For determining the concentration of bulk S in soil samples, it was >10 mg/kg. However, the S isotope composition of individual sulfur species could be analyzed if more than 1 mg of extract in the form of $BaSO_4$ was obtained.

3. Results and Discussion

3.1. Mineral Compositions

The mineralogical composition of the coal, the resulting ash, and the surrounding soil is summarized in Table 2. The coal mineral fraction is dominated by calcite ($CaCO_3$; ~70%) and dolomite ($CaMg(CO_3)_2$; ~20%), with small amounts (<10%) of gypsum ($CaSO_4 \cdot 2H_2O$) and pyrite (FeS_2), indicating deposition in a marine carbonate environment [7,9,32]. In contrast, the ash shows a more diverse mineralogical assemblage formed through multistage thermal decomposition and phase transformation during combustion. Calcite remains the dominant phase (~50%), accompanied by anhydrite ($CaSO_4$; ~30%) and aragonite ($CaCO_3$; ~5%). Additional phases (<10%) include periclase (MgO), portlandite ($Ca(OH)_2$), magnesite ($MgCO_3$), gypsum, barite ($BaSO_4$), and bassanite ($CaSO_4 \cdot 0.5H_2O$). This is consistent with the findings of Lieberman et al. [10].

Table 2. XRD determined the mineralogical composition of coal, ash, and soil samples.

Mineral	Coal	Ash	Soil
Calcite ($CaCO_3$)	~70%	~50%	
Dolomite ($CaMg(CO_3)_2$)	~20%		
Anhydrite ($CaSO_4$)		~30%	
Aragonite ($CaCO_3$)		~5%	
Gypsum ($CaSO_4 \cdot 2H_2O$)	<3%	<3%	
Pyrite (FeS_2)	<3%		
Periclase (MgO)		<3%	
Portlandite ($Ca(OH)_2$)		<3%	
Magnesite ($MgCO_3$)		<3%	
Barite ($BaSO_4$)		<3%	
Bassanite ($CaSO_4 \cdot 0.5H_2O$)		<3%	
Quartz (SiO_2)			~70%
Muscovite/Illite *			~25%
Albite ($NaAlSi_3O_8$)			<3%

* $KAl_2(AlSi_3O_{10})(OH)_2/K_{0.65}Al_{2.0}[Al_{0.65}Si_{3.35}O_{10}](OH)_2$.

XRD analysis of the soil near the Plomin TPP reveals a mineralogical composition dominated mainly by quartz (SiO_2; ~70%), followed by muscovite ($KAl_2(AlSi_3O_{10})(OH)_2$)/illite

($K_{0.65}Al_{2.0}[Al_{0.65}Si_{3.35}O_{10}](OH)_2$; ~25%) with albite ($Na(AlSi_3O_8)$) present as a minor phase. According to the pedological map of Istria [33], soils in the study area are predominantly classified as rendzinas, developed on carbonate bedrock, most commonly limestone and dolomite. The analyzed soil sample shows a pronounced depletion of carbonate minerals and a relative enrichment in silicate phases, indicating typical carbonate dissolution and soil formation from insoluble residua and possible eolian contribution [34]. The mineralogical signature is also consistent with terra rossa type soils in Istria [25].

3.2. Sulfur in Coal and Ash

The content of S and its stable isotope composition in coal and ash are presented in Table 3. The total S content in the coal and in all six coal samples is very high, exceeding 6.5 wt.%. According to Chou (2012) [8], these can be classified as the super-high organic sulfur (SHOES) coal group. The highest measured S content was 13.05 wt.%, while the average value was 8.73 wt.% (Table 3), which falls within the range of previous detailed analyses of Raša coal [9]. Earlier studies [7–9] showed that the average S content in Raša coal was 10.77 wt.%, with most of the S occurring as organically bound S (10.45 wt.%) and only a small part of the S as pyrite (0.3–0.63 wt.%) and sulfate (0.02 wt.%) [10].

Table 3. Content of S and isotopic composition of S in Raša coal and ash.

Sample	S (wt.%)	$\delta^{34}S$ (‰)
coal VIII/20	13.05	−5.50
coal VIII/99	6.50	−7.10
coal VIII/112	8.50	−5.80
coal 07	9.00	−9.20
coal 15	7.30	−6.20
coal 61	8.00	−9.60
min	7.30	−9.60
max	9.00	−5.80
average	8.73	−7.23
ash P–18	9.20	−3.51
ash P33	11.30	−3.38
ash P2	10.24	−3.49
min	9.20	−3.51
max	11.30	−3.49
average	10.25	−3.46

A high proportion of organic S in the coal is typical of the marine environment of coal formation [35], which was depleted in reactive Fe^{2+} and rich in sulfate compared to continental freshwater coal basins. The high S content was probably also influenced by the alkaline marine environment, which is very favorable for the incorporation of S into organic sedimentary substances, due to the high content of H_2S and HS^- [6,9].

The total sulfur contents in coal and ash were within the previously reported range (Table 3) [12]. The total S content in the ash is similar to or slightly higher than that in the coal samples (9.20–11.30 wt.%, average 10.25 wt.%; Table 3), except for the most S-rich sample (coal VIII/20). Considering the reported ash content of 10–24 wt.% in Raša coal [9,32], these results indicate incomplete combustion with only partial conversion of coal-bound S to SO_2. The relatively high S content in the ash suggests that a substantial fraction of sulfur is retained during combustion, and this retention is governed by several concurrent mechanisms.

An important factor is the incomplete release of sulfur from the mineral and organic matrix during combustion. Sulfur in coal exists in three main forms: (a) organic sulfur,

which predominates in Raša coal; (b) inorganic reduced sulfur, mostly as pyrite and marcasite; and (c) sulfates, typically associated with metals such as calcium and iron. Although organic sulfur, which is dominant in Raša coal, is largely released as gaseous species (H_2S, SO_2, CS_2) during devolatilization, some remains trapped in the char and is gradually released later during char burnout. Additionally, some coal-bound S may remain in the mineral phase due to self-retention, contributing to S retention in ash.

Besides incomplete release from the coal matrix, S released to the gas phase may be retained through reactions with alkaline compounds present in the ash. Coal contains certain amounts of alkali and alkaline earth metal compounds that form oxides during combustion and remain in the ash, where they can absorb S-bearing gases [36,37]. Calcium plays a particularly important role in this process, even in Raša coal, due to its high calcite content [9,10], which promotes the formation of calcium sulfate and enhances S retention in ash.

Iron oxides play a minor role in this process, as reflected by their absence in the ash, which is consistent with the low abundance of pyrite in Raša coal [38,39], indicating that Fe-bearing phases contribute little to S retention in this system. Overall, these processes indicate a complex S retention behavior involving both incomplete release from the mineral and organic phases and gas-phase reactions with ash constituents.

Most of the S in the ash is present as sulfate, while the remaining fraction may be retained in organic forms due to incomplete oxidation [40–43]. Nevertheless, the difference between bulk and sulfate-S in the ash in our samples cannot be explained solely by residual organically bound S and is most likely also influenced by incomplete dissolution of sulfate during elution.

3.3. Sulfur in Soil

The contents of the S species and their stable isotopic composition are shown in Table 4. The average S content in the vicinity of the Plomin TPP is 0.5 wt.% and is significantly higher than the average S content in agricultural soils, which is 0.03 wt.% [44,45]. The elemental analysis showed severe pollution with S. The average S content of the soil samples from the SW direction is about 13.75 times higher than at the control site (C1; 0.04 wt.%). This is mainly due to the highly S-enriched samples 19, 20, 21, and 22, which are closest to the TPP (100–400 m) along the PG line. The bulk S concentration in the SW soil sample at 100 m distance is almost 4 wt.%, which is approximately 100 times higher than at the control site. S contamination decreases rapidly to less than 0.2 wt.% at a distance of 5 km (Figure 4). A similar trend was observed for polycyclic aromatic hydrocarbons (PAHs) and potentially toxic metals such as Cu, V, and Zn [12].

Due to the limited number of valid observations (n = 8), we used a non-parametric Spearman Rank Order correlation to assess the relationships among distance, total sulfur content (S_{tot}), and sulfur isotopic composition ($\delta^{34}S$) (Table 5). The analysis revealed a strong and statistically significant negative correlation between distance and total S (S_{tot}; $\rho = -0.91$, $p < 0.05$), indicating that S content decreases as distance increases. Similarly, total S was strongly negatively correlated with $\delta^{34}S$ values ($\rho = -0.98$, $p < 0.05$), suggesting that lower S contents are associated with higher isotopic enrichment. In contrast, $\delta^{34}S$ showed a significant positive correlation with distance ($\rho = 0.90$, $p < 0.05$), reflecting the progressive isotopic enrichment of S with increasing distance from the source. These results highlight consistent spatial trends in both S content and isotopic composition across the study area.

Table 4. Contents and isotope composition (where applicable) of total S (S_{tot}), sulfate (S_{SO4}), and organically bound S in fulvic acid (S_{FA}) and humic acid (S_{HA}) in the soil at the PG line in SW direction from the Plomin TPP and in the control site C1.

Sample	D	Dist. (m)	S_{tot} (wt.%)	$\delta^{34}S_{tot}$ (‰)	S_{SO4} (wt.%)	$\delta^{34}S_{SO4}$ (‰)	S_{FA} (wt.%)	$\delta^{34}S_{FA}$ (‰)	S_{HA} (wt.%)	$\delta^{34}S_{HA}$ (‰)
19	SW	100	4.108	/	/	/	/	/	/	/
20	SW	200	1.110	/	0.0009	/	0.019	+4.2	0.801	−3.2
21	SW	300	1.112	+1.71	0.003	+1.7	0.027	+5.8	0.601	−3.6
22	SW	400	1.365	+0.81	0.0051	+0.8	0.019	+4.8	0.522	+5.9
28	SW	1000	0.524	+5.54	0.0014	+5.5	0.011	/	/	/
1.5 KM	SW	1500	0.220	+7.90	bd	/	0.005	/	0.347	/
2 KM	SW	2000	0.180	+11.50	bd	/	0.001	/	0.192	/
3 KM	SW	3000	0.140	+17.40	bd	/	/	/	/	/
4 KM	SW	4000	0.130	+20.02	bd	/	/	/	/	/
5 KM	SW	5000	0.190	+11.90	bd	/	0.002	/	0.241	/
C1	NE	>10,000	0.036	/	bd	/	bd	/	bd	/
1 KM	NW	1000	0.160	+24.80	bd	/	/	/	/	/

bd—below detection limit; /—to small quantity of the sample or not enough total S for further analysis.

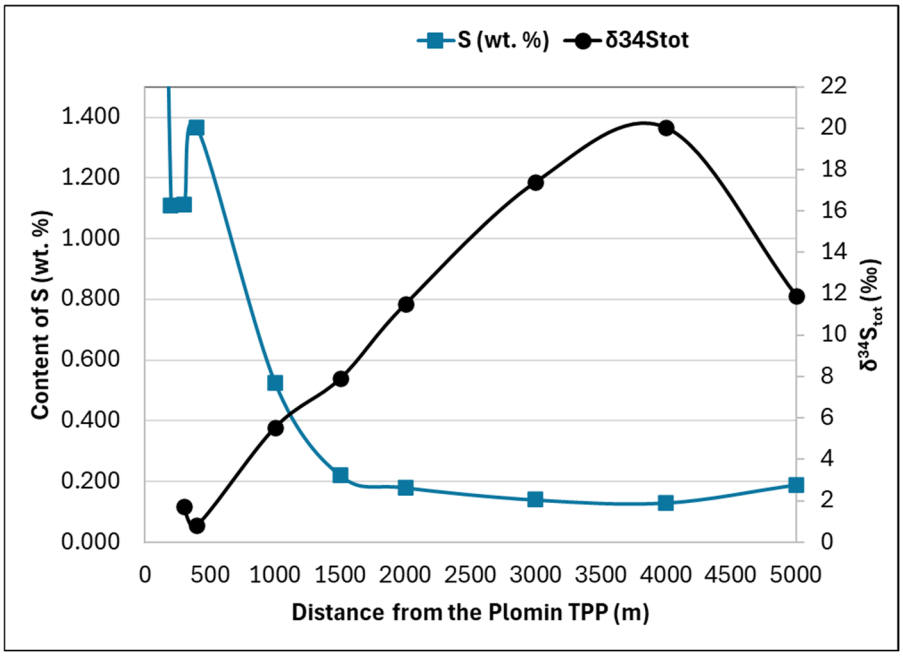

Figure 4. Relation between content and isotopic composition of S in soil and distance from the Plomin TPP.

Table 5. Spearman Rank Order correlation coefficients between distance, total sulfur content (S_{tot}), and $\delta^{34}S$. Correlations are statistically significant at $p < 0.05$.

Variable	Distance	S_{tot}	$\delta^{34}S$
Distance	1.0	−0.91	0.90
S_{tot}	−0.91	1.0	−0.98
$\delta^{34}S$	0.90	−0.98	1.0

The analysis of forest soils similar to those from the Raša area [46] showed that S accumulation in soils is believed to be higher near industrial sources, as 98% of industrially emitted S enters the atmosphere in the form of SO_x, some of which is readily converted to sulfate aerosols and deposited through wet and dry deposition. Some of this gas is then

assimilated and captured by plants. The removal of SO_2 depends on local atmospheric dynamics and tree density [46]. Cicek and Koparal [47] reported the opposite trend near the Tunçbilek thermal power plant in Turkey—an increase in soil S content with increasing distance from the TPP, which they explained by the high chimney of the TPP and the resulting greater dispersion of the emitted SO_2.

A comparison of soil samples from our study area, taken in the wind direction with those from the opposite direction showed that the prevailing wind direction strongly influences the distribution of S. In principle, a moderately elevated S content in soil is not problematic for long-term plant growth, unless the values are extremely high, such as. in saline soils or in areas where sulfate from the atmosphere is deposited in excessive amounts due to anthropogenic pollution and the soil remains acidic, which is not the case in our carbonate-rich soils [48].

Only a small part of the S in the soil remained bound in the form of sulfate. At a distance of 1.5 km or more, its content was below the detection limit. Further speciation analysis showed that organically bound S predominated in all but one sample at 400 m SW from the TPP, where more than half of the total S (S_{tot}) remained unaccounted for. The mean S content bound to humic acids (0.45 wt.%) is approximately 37.5 times greater than the mean S content bound to fulvic acids (0.012 wt.%). The ratio between inorganic and organically bound S corresponds to the S content in most agricultural soils [49]. Inorganic S is usually much less abundant, representing 10% or less of the total soil S [50]. These transformation processes are central to understanding the long-term fate of sulfur and its implications for sustainable soil management at historically contaminated sites. It was shown that sulfate can be directly incorporated into soil organic matter, forming complex compounds such as amino acids, sulfonates, ester sulfates, and others [51,52]. Sulfurization of organic matter and organosulfur degradation thus act as an integral link between the organic and inorganic sulfur pools [53], helping to maintain S levels in soil over time by balancing inputs (i.e., atmospheric deposition, predominantly composed of sulfate-S), and assimilation of S by microbes or plants, and the leaching of S forms in soils [54].

From this, we conclude that in the 20 years since Raša coal has no longer been used, the majority of deposited S was either incorporated into soil organic matter by microbial sulfurization or recycled by plants, which then returns to the soil as organosulfur compounds or in mineral form through decomposition and mineralization [50,55]. The low sulfate content with positive $\delta^{34}S$ values, despite high total S content in soils, suggests relatively rapid recycling of bioavailable sulfate rather than washout of easily soluble sulfate from the soil, even though [55] leaching is much faster than assimilation, particularly during periods of moderate to high precipitation [56,57]. Although total S content in the soil within 2 km of the TPP remained high, most of the S was transferred to the organic S pool, which becomes available to plants only through mineralization [54].

Although current findings suggest that sulfate may no longer be a potential environmental threat, this conclusion should be approached with caution. A large portion of the S in the soil near the Plomin TPP is bound in organic forms. This is consistent with global observations of sulfur distribution in soil, where the majority (>95%) of S is bound to organic matter, particularly humic and fulvic substances [58], while the remainder is present as sulfide (S^{2-}), sulfate ($SO_4{}^{2-}$), and elemental sulfur (S^0) [59]. Although organically bound S is not directly bioavailable, it represents a dynamic reservoir that can be remobilized through mineralization processes over time [60–63]. The rate of organosulfur mineralization is strongly influenced by environmental changes, including shifts in microbial community composition, redox conditions, soil moisture, temperature, and land use. These processes may result in the delayed release of sulfate, potentially causing soil acidification, nutrient imbalances, and leaching into groundwater. Even though the current risk appears low,

it is important to continue monitoring to understand the stability of these organic sulfur compounds and their possible future effects.

Therefore, although the current risk associated with sulfate appears low, long-term monitoring is recommended. Such monitoring is essential to assess the stability of organically bound sulfur under changing environmental conditions and to better predict its potential ecological impact over time. From a sustainability perspective, these findings highlight the importance of considering sulfur speciation and long-term monitoring when evaluating the efficiency of natural attenuation at legacy pollution sites.

3.4. Isotopic Composition of Sulfur

The stable S isotope composition of anthropogenic emissions generally shows a wide range of values depending on the nature of sources. The δ^{34}S values of bulk Raša coal samples are negative, ranging from −5.5 to −9.5‰ (Table 3). Coal is generally characterized by a broad range of δ^{34}S values, from −35 to +30‰, with coals containing high S content usually showing more negative δ^{34}S values. This is due to microbial sulfate reduction during the biochemical transformation of organic matter and the transfer of ^{34}S-depleted reduced S into the organic matter [64–66]. The δ^{34}S values of the ash in all three samples are around −3.5 ‰ and are slightly higher than those in the coal. This is consistent with the S isotope fractionation during coal combustion reported in the literature, where effluents and fly ash from coal combustion exhibit the same or higher δ^{34}S values than the coal [43,65,67]. Overall, the S contained in ashes is enriched in ^{34}S compared to the coal, leading to the conclusion that the bulk airborne S emissions should have negative δ^{34}S values, lower than those of the bulk S in coal.

The δ^{34}S values of bulk soil samples range from +0.8 to nearly +25‰ and increase with distance from the TPP. The δ^{34}S values of humic substances range from −3.5 to 5.9‰, while S in fulvic acids shows positive values between +4.2 and +5.8‰. Obviously, regarding the bulk S isotope composition and the sulfur mass balance, a considerable part of S species remained unaccounted for. The processes of sulfurization of organic matter are generally associated with a S isotope fractionation of 3–5‰, where both oxidized and reduced S species can be incorporated into the organic substrate [68,69]. Although sulfurization of organic matter is typical in anoxic environments [70], it can also occur in oxidizing environments, including carbonate-rich soils, where intermediate and oxidized S species are added to the organic substrates during microbially mediated diagenetic recycling of sulfur [28,68,71]. On the other hand, the assimilation of sulfate into plants is associated with a smaller S isotope fractionation, as sulfate depleted in ^{34}S by 1–2‰ is assimilated. This leads to enrichment of the remaining sulfate pool in ^{34}S, for example, at the site 1 km NW of the TPP [57,72].

The dominant source of S in the soil close to the Plomin TPP is obviously still the historical airborne S emissions from the Plomin TPP, which contributed ^{34}S-depleted S in addition to sea spray-derived sulfate (with an average δ^{34}S value of approximately +21‰) [73]. The increasing trend of δ^{34}S values and the decreasing S content with distance from the TPP (Table 4, Figure 4) indicate a decreasing anthropogenic S input into the soils. Total S content decreased from 1.112 wt.% near the TPP to 0.19 wt.% at a distance of 5 km, yet remained higher than at the control site C1 (0.036 wt.%). In contrast, δ^{34}S values increased from +1.71 to 20.02 with distance, approaching values characteristic of marine sulfate, indicating a diminishing influence of airborne contamination from the Plomin TPP and an increasing contribution of sea spray sulfate. This divergence between content and isotopic trends suggests that isotopic signatures may approach background values earlier than sulfur content, reflecting the persistence of residual sulfur in soils despite reduced isotopic evidence of anthropogenic inputs.

This distance therefore could represent the approximate limit of notable anthropogenic sulfur pollution, even 20 years after the cessation of high-S emissions. At a distance of 4 km in the southwest (SW) direction, the isotopic composition of S in the soil is very similar to the isotopic composition of marine sulfate. The site 5 km from the TPP had a similarly low bulk S content but a lower δ^{34}S value, similar to the site at 2 km (Table 4). Local air circulation and the hilly topography may have caused an irregular distribution of flue gas and aerosols from the TPP. However, the observed isotopic patterns are more likely influenced by biological sulfur turnover in soil, which can produce a similar isotope effect over time [71,73].

4. Conclusions

In this study, the sulfur content and isotopic composition of S in soils around the Plomin TPP were determined 20 years after the cessation of high-sulfur emissions from Raša coal combustion. The following conclusions can be drawn:

(1) The spatial distribution of sulfur contamination in the soil is closely related to the distance from the Plomin TPP and is strongly influenced by the prevailing wind direction (SW). The sulfur content in the soil decreases with distance along the pollution gradient (PG) from the Plomin TPP, reaching background levels more than 10 km away in the NE direction (control site C1), consistent with typical agricultural soils (0.03 wt.%).

(2) Sulfur speciation in soil reveals the dominance of organically bound sulfur (>98%), primarily associated with humic acids (>95%). The low proportion of sulfate indicates rapid microbial assimilation and transformation of sulfur into organic form. This suggests that natural processes have efficiently reduced sulfate levels in the soil since emissions ceased.

(3) The S isotopic composition (δ^{34}S) varies with distance from the Plomin TPP, confirming that ^{34}S-depleted emissions from Raša coal combustion were the primary source of anthropogenic contamination. Increasing δ^{34}S values with distance suggest an increasing influence of marine sulfate and natural soil processes.

(4) These findings demonstrate that the legacy of sulfur pollution can persist in organic forms long after emissions cease, with important implications for long-term soil biogeochemistry. Although current sulfate levels are low, residual organic sulfur may still undergo mineralization and potentially release sulfate under changing environmental conditions. Due to the elevated sulfur content in the soil, continued monitoring is necessary to assess potential environmental impacts and long-term changes.

(5) The observed transformation of sulfur forms highlights the role of natural attenuation in enhancing long-term soil resilience and provides a scientific basis for the sustainable management of sites historically affected by anthropogenic atmospheric sulfur deposition.

Author Contributions: The lead author of this study is N.M.A. Conceptualization, N.M.A.; methodology, S.L. and N.M.A.; validation, N.M.A., S.L. and N.Z.; investigation, N.M.A., S.L. and N.Z.; resources, S.L.; writing—original draft preparation, N.M.A.; writing—review and editing, S.L. and N.Z.; visualization, N.M.A.; supervision, S.L., and N.Z. All authors have read and agreed to the published version of the manuscript.

Funding: This research was funded by Slovenian Research and Innovation Agency ARIS, programs P1–0143, P1-0025 and P1-0008.

Institutional Review Board Statement: Not applicable.

Informed Consent Statement: Not applicable.

Data Availability Statement: The original contributions presented in this study are included in the article. Further inquiries can be directed to the corresponding author.

Acknowledgments: The authors gratefully acknowledge Gordana Medunić from the Faculty of Science, University of Zagreb, Croatia, for initiating this research and for providing the samples, without which this study would not have been possible. We also thank Stojan Žigon (Jožef Stefan Institute) for valuable analytical support and Matej Dolenec (Dept. of Geology, Faculty of Natural Sciences and Engineering, University of Ljubljana) for performing the X-ray diffraction (XRD) analyses. We gratefully appreciate the financial support of the Slovenian Research and Innovation Agency (ARIS). We would also like to express our sincere gratitude to the reviewers for their constructive comments, insightful suggestions, and careful evaluation, which significantly improved the quality of this manuscript.

Conflicts of Interest: The authors declare no conflicts of interest.

References

1. Wedepohl, K.H. The composition of the continental crust. *Geochim. Cosmochim. Acta* **1995**, *59*, 1217–1232. [CrossRef]
2. Rudnick, R.L.; Gao, S. Composition of the Continental Crust. In *Treatise on Geochemistry*, 2nd ed.; Holland, H.D., Turekian, K.K., Eds.; Elsevier Science: Amsterdam, The Netherlands, 2003; Volume 4.1, pp. 1–51.
3. Balík, J.; Kulhánek, M.; Černý, J.; Száková, J.; Pavlíková, D.; Čermák, P. Differences in soil sulfur fractions due to limitation of atmospheric deposition. *Plant Soil Environ.* **2009**, *55*, 344–352. [CrossRef]
4. Sharma, R.K.; Cox, M.S.; Oglesby, C.; Dhillon, J.S. Revisiting the role of sulfur in crop production: A narrative review. *J. Agric. Food Res.* **2024**, *15*, 101013. [CrossRef]
5. International Energy Agency. Available online: https://www.iea.org/ (accessed on 10 November 2025).
6. Medunić, G.; Rađenović, A.; Bajramović, M.; Švec, M.; Tomac, M. Once grand, now forgotten: What do we know about the superhigh-organic-sulphur Raša coal? *Rud.-Geološko-Naft. Zb.* **2016**, *31*, 27–45. [CrossRef]
7. White, C.M.; Douglas, L.J.; Anderson, R.R.; Schmidt, C.E.; Gray, R.J. Organosulfur Constituents in Rasa Coal. In *Geochemistry of Sulfur in Fossil Fuels*; Orr, W.L., White, C.M., Eds.; American Chemical Society: Washington, DC, USA, 1990; Volume 429, pp. 261–286.
8. Chou, C.L. Sulfur in coals: A review of geochemistry and origins. *Int. J. Coal Geol.* **2012**, *100*, 1–13. [CrossRef]
9. Medunić, G.; Grigore, M.; Dai, S.; Berti, D.; Hochella, M.F.; Mastalerz, M.; Valentim, B.; Guedes, A.; Hower, J.C. Characterization of superhigh-organic-sulfur Raša coal, Istria, Croatia, and its environmental implication. *Int. J. Coal Geol.* **2020**, *217*, 103344. [CrossRef]
10. Lieberman, N.R.; Izquierdo, M.; Muñoz-Quirós, C.; Cohen, H.; Chenery, S.R. Geochemical signature of superhigh organic sulphur Raša coals and the mobility of toxic trace elements from combustion products and polluted soils near the Plomin coal-fired power station in Croatia. *Appl. Geochem.* **2020**, *114*, 104472. [CrossRef]
11. Marović, G.; Senčar, J.; Kovač, J.; Prlić, I. Improvement of the radiological environmental situation due to remedial actions at a coal-fired power plant. *J. Radioanal. Nucl. Chem.* **2004**, *261*, 451–455. [CrossRef]
12. Medunić, G.; Ahel, M.; Mihalić, I.B.; Srček, V.G.; Kopjar, N.; Fiket, Ž.; Bituh, T.; Mikac, I. Toxic airborne S, PAH, and trace element legacy of the superhigh-organic-sulphur Raša coal combustion: Cytotoxicity and genotoxicity assessment of soil and ash. *Sci. Total Environ.* **2016**, *566–567*, 306–319. [CrossRef]
13. Lovrenčić Mikelić, I.; Ernečić, G.; Barišić, D. Natural and anthropogenic radionuclides in soil around coal-fired Plomin thermal power plant (Istria, Croatia): What is the plant influence and what controls it? *Fuel* **2024**, *371*, 131971. [CrossRef]
14. Medunić, G.; Mihalić, I.B.; Ahel, M.; Mikac, I.; Kopjar, N.; Srček, V.G. Toxicity risk assessment of sulfur and PAHs in soil surrounding a coal-fired power plant. In Proceedings of the 27th International Applied Geochemistry Symposium, Tucson, AZ, USA, 20–24 April 2015; pp. 1–17.
15. Miko, S.; Durn, G.; Adamcová, R.; Čović, M.; Dubíková, M.; Skalský, R.; Kapelj, S.; Ottner, F. Heavy metal distribution in karst soils from Croatia and Slovakia. *Environ. Geol.* **2003**, *45*, 262–272. [CrossRef]
16. Peh, Z.; Miko, S.; Hasan, O. Geochemical background in soils: A linear process domain? An example from Istria (Croatia). *Environ. Earth Sci.* **2010**, *59*, 1367–1383. [CrossRef]
17. Orešcanin, V.; Franekic-Colic, J.; Durgo, K.; Valkovic, V. Investigation of mutagenic effect of metals in the plomin bay sediments by modified preincubation ames assay. *J. Trace Microprobe Tech.* **2002**, *20*, 69–77. [CrossRef]
18. Mohorovic, L. First two months of pregnancy—Critical time for preterm delivery and low birthweight caused by adverse effects of coal combustion toxics. *Early Hum. Dev.* **2004**, *80*, 115–123. [CrossRef]

19. Mohorovic, L. The level of maternal methemoglobin during pregnancy in an air-polluted environment. *Environ. Health Perspect.* **2003**, *111*, 1902–1905. [CrossRef]
20. Cesar, V.; Užarević, Z.; Potočić, N.; Seletković, I.; Lepeduš, H. Preliminary report on epicuticular wax structure in Black pine needles affected by SO_2 emitted from thermal power plant Plomin (Croatia). *Period. Biol.* **2005**, *107*, 357–360.
21. Radić, S.; Medunić, G.; Kuharić, Ž.; Roje, V.; Maldini, K.; Vujčić, V.; Krivohlavek, A. The effect of hazardous pollutants from coal combustion activity: Phytotoxicity assessment of aqueous soil extracts. *Chemosphere* **2018**, *199*, 191–200. [CrossRef]
22. Gutiérrez, F.; Parise, M.; De Waele, J.; Jourde, H. A review on natural and human-induced geohazards and impacts in karst. *Earth-Sci. Rev.* **2014**, *138*, 61–88. [CrossRef]
23. Parise, M.; Gunn, J. Natural and anthropogenic hazards in karst areas: An introduction. *Geol. Soc. Lond. Spec. Publ.* **2007**, *279*, 1–3. [CrossRef]
24. Vlahović, I.; Tišljar, J.; Velić, I.; Matičec, D. Evolution of the Adriatic Carbonate Platform: Palaeogeography, main events and depositional dynamics. *Palaeogeogr. Palaeoclimatol. Palaeoecol.* **2005**, *220*, 333–360. [CrossRef]
25. Durn, G.; Ottner, F.; Slovenec, D. Mineralogical and geochemical indicators of the polygenetic nature of terra rossa in Istria, Croatia. *Geoderma* **1999**, *91*, 125–150. [CrossRef]
26. The Global Wind Atlas. Available online: https://globalwindatlas.info/en/ (accessed on 10 November 2025).
27. Brüchert, V.; Pratt, L.M. Contemporaneous early diagenetic formation of organic and inorganic sulfur in estuarine sediments from St. Andrew Bay, Florida, USA. *Geochim. Cosmochim. Acta* **1996**, *60*, 2325–2332. [CrossRef]
28. Lojen, S.; Čermelj, B.; Wartel, M. Sulfur cycling and the sulfurization of humic and fulvic acids in the sediments of the rivers Rupel (Belgium) and Authie (northern France). *Oceanol. Hydrobiol. Stud.* **2007**, *36*, 83–101. [CrossRef]
29. Mott, R.A.; Wilkinson, H.C. The use of the Eschka method for the determination of high sulphur contents. *J. Appl. Chem.* **1953**, *3*, 218–223. [CrossRef]
30. USGS Laboratory Management System (LIMS). Available online: https://water.usgs.gov/water-resources/software/RSIL-LIMS/ (accessed on 13 November 2025).
31. Halas, S.; Szaran, J. Improved thermal decomposition of sulfates to SO_2 and mass spectrometric determination of $\delta^{34}S$ of IAEA SO-5, IAEA SO-6 and NBS-127 sulfate standards. *Rapid Commun. Mass Spectrom.* **2001**, *15*, 1618–1620. [CrossRef]
32. Valković, V.; Makjanić, J.; Jaksić, M.; Popović, S.; Bos, A.J.J.; Vis, R.D.; Wiederspahn, K.; Verheul, H. Analysis of fly ash by X-ray emission spectroscopy and proton microbeam analysis. *Fuel* **1984**, *63*, 1357–1362. [CrossRef]
33. Škorić, A.; Mayer, B.; Vranković, A.; Bašić, F. *Pedološka Karta Istre 1:150,000*; Projektni Zavod za Izradu Pedološke Karte SR Hrvatske: Zagreb, Croatia, 1983.
34. Zupančič, N.; Turniški, R.; Miler, M.; Grčman, H. Geochemical fingerprint of insoluble material in soil on different limestone formation. *CATENA* **2018**, *170*, 10–24. [CrossRef]
35. Dai, S.; Finkelman, R.B.; Hower, J.C.; French, D.; Graham, I.T.; Zhao, L. *Inorganic Geochemistry of Coal*, 1st ed.; Elsevier: Amsterdam, The Netherlands, 2023; p. 438.
36. Spörl, R.; Maier, J.; Scheffknecht, G. Sulphur oxide emissions from dust-fired oxy-fuel combustion of coal. *Energy Procedia* **2013**, *37*, 1435–1447. [CrossRef]
37. Müller, M.; Schnell, U.; Scheffknecht, G. Modelling the fate of sulphur during pulverized coal combustion under conventional and oxy-fuel conditions. *Energy Procedia* **2013**, *37*, 1377–1388. [CrossRef]
38. Vassileva, C.G.; Vassilev, S.V. Behaviour of inorganic matter during heating of Bulgarian coals: 1. Lignites. *Fuel Process. Technol.* **2005**, *86*, 1297–1333. [CrossRef]
39. Huang, F.; Xin, S.; Mi, T.; Zhang, L. Investigation on the transformation behaviours of Fe-bearing minerals of coal in O_2/CO_2 combustion atmosphere containing H_2O. *RSC Adv.* **2021**, *11*, 10635–10645. [CrossRef]
40. Wei, Q.; Song, W. Mineralogical and Chemical Characteristics of Coal Ashes from Two High-Sulfur Coal-Fired Power Plants in Wuhai, Inner Mongolia, China. *Minerals* **2020**, *10*, 323. [CrossRef]
41. Shao, P.; Hou, H.; Wang, W.; Wang, W. Geochemistry and mineralogy of fly ash from the high-alumina coal, Datong Coalfield, Shanxi, China. *Ore Geol. Rev.* **2023**, *158*, 105476. [CrossRef]
42. Wilcox, J.; Wang, B.; Rupp, E.; Taggart, R.; Hsu-Kim, H.; Oliveira, M.L.S.; Cutruneo, C.M.N.L.; Taffarel, S.; Silva, L.F.O.; Hopps, S.D.; et al. Observations and Assessment of Fly Ashes from High-Sulfur Bituminous Coals and Blends of High-Sulfur Bituminous and Subbituminous Coals: Environmental Processes Recorded at the Macro- and Nanometer Scale. *Energy Fuels* **2015**, *29*, 7168–7177. [CrossRef]
43. Shen, Y.; Zhang, Q.; Xu, Y.; Thiemens, M.H. Sulfur isotope anomalies in coal combustion: Applications to the present and early Earth environments. *Proc. Natl. Acad. Sci. USA* **2024**, *121*, e2408199121. [CrossRef]
44. Aguilera, M.; De la Luz Mora, M.; Borie, G.; Peirano, P.; Zunino, H. Balance and distribution of sulphur in volcanic ash-derived soils in Chile. *Soil Biol. Biochem.* **2002**, *34*, 1355–1361. [CrossRef]

45. Reimann, C.; Demetriades, A.; Birke, M.; Filzmoser, P.; O'Connor, P.; Halamić, J.; Ladenberger, A. The GEMAS Project Team. Agricultural and grazing land soil of Europe. In *Chemistry of Europe's Agricultural Soils, Part A—Methodology and Interpretation of the GEMAS Data Set*, 1st ed.; Reimann, C., Birke, M., Demetriades, A., Filzmoser, P., O'Connor, P., Eds.; Schweizerbart Science Publishers: Stuttgart, Germany, 2014; pp. 101–472.
46. Novák, M.; Kirchner, J.W.; Fottová, D.; Přechová, E.; Jačková, I.; Krám, P.; Hruska, J. Isotopic evidence for processes of sulfur retention/release in 13 forested catchments spanning a strong pollution gradient (Czech Republic, central Europe). *Glob. Biogeochem. Cycles* **2005**, *19*. [CrossRef]
47. Cicek, A.; Koparal, A.S. Accumulation of sulfur and heavy metals in soil and tree leaves sampled from the surroundings of Tunçbilek Thermal Power Plant. *Chemosphere* **2004**, *57*, 1031–1036. [CrossRef]
48. Likus-Cieślik, J.; Pietrzykowski, M.; Chodak, M. Chemistry of sulfur-contaminated soil substrate from a former frasch extraction method sulfur mine leachate with various forms of litter in a controlled experiment. *Water Air Soil Pollut.* **2018**, *229*, 71. [CrossRef]
49. Tabatabai, M.A. Methods of measurement of sulphur in soils, plant materials and waters. In *Sulphur Cycling on the Continents—Wetlands, Terrestrial Ecosystems and Associated Water Bodies; SCOPE 48*; Howarth, R.W., Stewart, J.W.B., Ivanov, M.V., Eds.; John Wiley & Sons: New York, NY, USA, 1992.
50. Scherer, H.W. Sulphur in crop production—Invited paper. *Eur. J. Agron.* **2001**, *14*, 81–111. [CrossRef]
51. Strickland, T.C.; Fitzgerald, J.W. Incorporation of sulphate-sulphur into organic matter extracts of litter and soil: Involvement of ATP sulphurylase. *Soil Biol. Biochem.* **1985**, *17*, 779–784. [CrossRef]
52. Magnucka, E.; Kulczycki, G.; Oksińska, M.P.; Kucińska, J.; Pawęska, K.; Milo, L.; Pietr, S. The effect of various forms of sulfur on soil organic matter fractions and microorganisms in a pot experiment with perennial ryegrass (*Lolium perenne* L.). *Plants* **2023**, *12*, 2649. [CrossRef]
53. Patsis, A.C.; Schuler, C.J.; Toner, B.M.; Santelli, C.M.; Sheik, C.S. The potential for coupled organic and inorganic sulfur cycles across the terrestrial deep subsurface biosphere. *Nat. Commun.* **2025**, *16*, 3827. [CrossRef]
54. Fakhraee, M.; Li, J.; Katsev, S. Significant role of organic sulfur in supporting sedimentary sulfate reduction in low-sulfate environments. *Geochim. Cosmochim. Acta* **2017**, *213*, 502–516. [CrossRef]
55. Schroth, A.W.; Bostick, B.C.; Graham, M.; Kaste, J.M.; Mitchell, M.J.; Friedland, A.J. Sulfur species behavior in soil organic matter during decomposition. *JGR Biogeosci.* **2007**, *112*. [CrossRef]
56. Davidian, J.-C.; Kopriva, S. Regulation of sulfate uptake and assimilation--the same or not the same? *Mol. Plant* **2010**, *3*, 314–325. [CrossRef]
57. Cao, Y.W.; Wang, X.B.; Wang, C.; Bai, E.; Wu, N. Sulfur biogeochemical dynamics of grassland soils in northern China transect along an aridity gradient. *Geoderma* **2024**, *451*, 117073. [CrossRef]
58. Howarth, R.W.; Stewart, J.W.B.; Ivanov, M.V. *Sulphur Cycling on the Continents: Wetlands, Terrestrial Ecosystems, and Associated Waterbodies*; Chichester: New York, NY, USA, 1992; 350p.
59. Zenda, T.; Liu, S.; Dong, A.; Duan, H. Revisiting sulphur—The once neglected nutrient: It's roles in plant growth, metabolism, stress tolerance and crop production. *Agriculture* **2021**, *11*, 626. [CrossRef]
60. Edwards, P.J. *Sulfur Cycling, Retention, and Mobility in Soils: A Review; NE-250*; USDA Forest Service: Delaware, OH, USA, 1998; 18p.
61. Ranadev, P.; Ashwin, R.; Bagyaraj, D.J.; Shinde, A.H. Sulfur oxidizing bacteria in agro ecosystem and its role in plant productivity—A review. *J. Appl. Microbiol.* **2023**, *134*, lxad161. [CrossRef]
62. Churka Blum, S.; Lehmann, J.; Solomon, D.; Caires, E.F.; Alleoni, L.R.F. Sulfur forms in organic substrates affecting S mineralization in soil. *Geoderma* **2013**, *200–201*, 156–164. [CrossRef]
63. Xiao, H.Y.; Liu, C.Q. The elemental and isotopic composition of sulfur and nitrogen in Chinese coals. *Org. Geochem.* **2011**, *42*, 84–93. [CrossRef]
64. Chen, S.; Guo, Z.; Guo, Z.; Guo, Q.; Zhang, Y.; Zhu, B.; Zhang, H. Sulfur isotopic fractionation and its implication: Sulfate formation in $PM_{2.5}$ and coal combustion under different conditions. *Atmos. Res.* **2017**, *194*, 142–149. [CrossRef]
65. Thode, H.G. Sulphur isotopes in nature and the environment: An overview. In *SCOPE 43: Stable Isotopes: Natural and Anthropogenic Sulphur in the Environment Krouse*; Krouse, H.R., Grinenko, V.A., Eds.; John Wiley & Sons Ltd.: Hoboken, NJ, USA, 1991; pp. 1–26.
66. Jiang, Y.; Elswick, E.R.; Mastalerz, M. Progression in sulfur isotopic compositions from coal to fly ash: Examples from single-source combustion in Indiana. *Int. J. Coal Geol.* **2008**, *73*, 273–284. [CrossRef]
67. Canfield, D.E. Factors influencing organic carbon preservation in marine sediments. *Chem. Geol.* **1994**, *114*, 315–329. [CrossRef]
68. Amrani, A.; Aizenshtat, Z. Mechanisms of sulfur introduction chemically controlled: $\delta^{34}S$ imprint. *Org. Geochem.* **2004**, *35*, 1319–1336. [CrossRef]
69. Raven, M.R.; Fike, D.A.; Gomes, M.L.; Webb, S.M. Chemical and isotopic evidence for organic matter sulfurization in redox gradients around mangrove roots. *Front. Earth Sci.* **2019**, *7*, 98. [CrossRef]
70. Meija, J.; Coplen, T.B.; Berglund, M.; Brand, W.A.; De Bièvre, P.; Gröning, M.; Holden, N.E.; Irrgeher, J.; Loss, R.D.; Walczyk, T.; et al. Atomic weights of the elements 2013 (IUPAC Technical Report). *Pure Appl. Chem.* **2016**, *88*, 265–291. [CrossRef]

71. Alewell, C.; Gehre, M. Patterns of stable S isotopes in a forested catchment as indicators for biological S turnover. *Biogeochemistry* **1999**, *47*, 317–331. [CrossRef]
72. Tcherkez, G.; Tea, I. $^{32}S/^{34}S$ isotope fractionation in plant sulphur metabolism. *New Phytol.* **2013**, *200*, 44–53. [CrossRef]
73. Habicht, K.S.; Canfield, D.E.; Rethmeier, J. Sulfur isotope fractionation during bacterial reduction and disproportionation of thiosulfate and sulfite. *Geochim. Cosmochim. Acta* **1998**, *62*, 2585–2595. [CrossRef]